

Programmable Hierarchical Three-Component 2D Assembly at a Liquid-Solid interface: Recognition, Selection and Transformation

Shengbin Lei, Mathieu Surin, Kazukuni Tahara, Jinne Adisojoso, Roberto Lazzaroni, Yoshito Tobe, and Steven De Feyter

A. Compounds

B. Experimental Data: Scanning Tunneling Microscopy images

B.1. Scanning tunneling microscopy

B.2. Three-component 2D assembly of DBA1, ISA and COR

B.3. Assembly of binary mixture of DBA1 and ISA

B.4. Assembly of binary mixture of TMA and ISA

B.5. Assembly of ternary mixture of TMA, ISA and COR

B.6. Assembly of DBA1 in the presence of TMA and COR

C. Molecular Mechanics and Molecular Dynamics Simulations

C.1. Methodology

C.2. Table

C.3. The pure ISA monolayer : linear vs. hexagonal H-bonded networks

C.4. The two-component monolayer : COR/ISA

C.5. The three-component monolayer : DBA/COR/ISA

A. Compounds

Isophthalic acid, 1,3,5-trimesic acid, octanoic acid and coronene are purchased from Acros Co. Syntheses of **DBA1** and **DBA2** were reported previously.¹

B. Experimental Data: Scanning Tunneling Microscopy Images

B.1. Scanning tunnelling microscopy

For STM measurements, **ISA**, **TMA** or **COR** are dissolved separately into octanoic acid (saturated). **DBA1** and **DBA2** are dissolved into octanoic acid with concentrations ranging from 8×10^{-4} mol/L to 8×10^{-6} mol/L. A drop of a solution is applied on a freshly-cleaved graphite substrate (HOPG, grade ZYB, Advanced Ceramics Inc., Cleveland, USA). STM images were acquired using a PicoSPM (Agilent) operating in constant current mode with the tip immersed in the solution at room temperature (21–22 °C). Pt/Ir (80/20%) tips were prepared by mechanical cutting. The graphite lattice was recorded by lowering the bias immediately after obtaining images of the assembly. The drift of the image was corrected using the Scanning Probe Image Processor (SPIP) software (Image Metrology ApS) against the graphite lattice.

B.2. Three-component 2D assembly of DBA1, ISA and COR

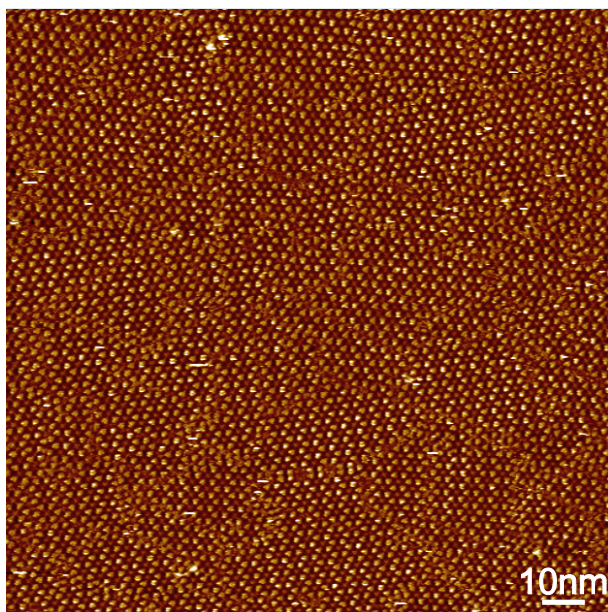


Figure S1. Large scale STM images at the 1-octanoic acid/graphite interface of the hierarchical assembly of **DBA1** with **ISA** and **COR**. Several domains are observed $I_{\text{set}} = 58$ pA, $V_{\text{set}} = -1.04$ V; Concentration: **DBA1**, 8×10^{-5} mol/L, **ISA** and **COR**, saturated.

B.3. Assembly of binary mixture of DBA1 and ISA

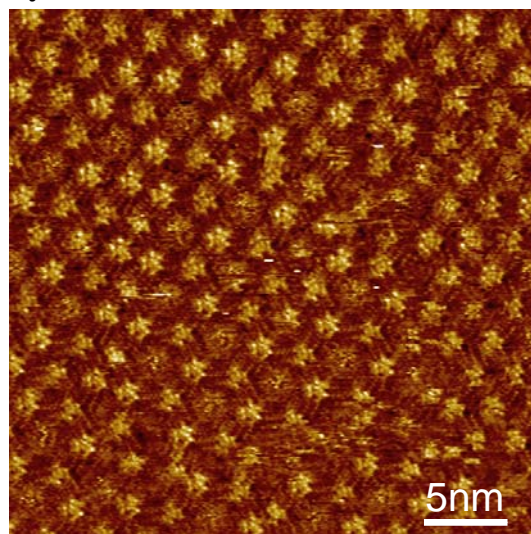


Figure S2. STM image at the 1-octanoic acid/graphite interface of a mixture of **ISA** and **DBA1**. The presence of **ISA** has no effect on the **DBA1** network and there is no evidence for the formation of cyclic **ISA** hexamers in the **DBA1** pores in absence of **COR**. $I_{\text{set}} = 33 \text{ pA}$; $V_{\text{set}} = 1.04 \text{ V}$; Concentration: **DBA1**, $8 \times 10^{-5} \text{ mol/L}$, **ISA**, saturated.

B.4. Assembly of binary mixture of TMA and ISA

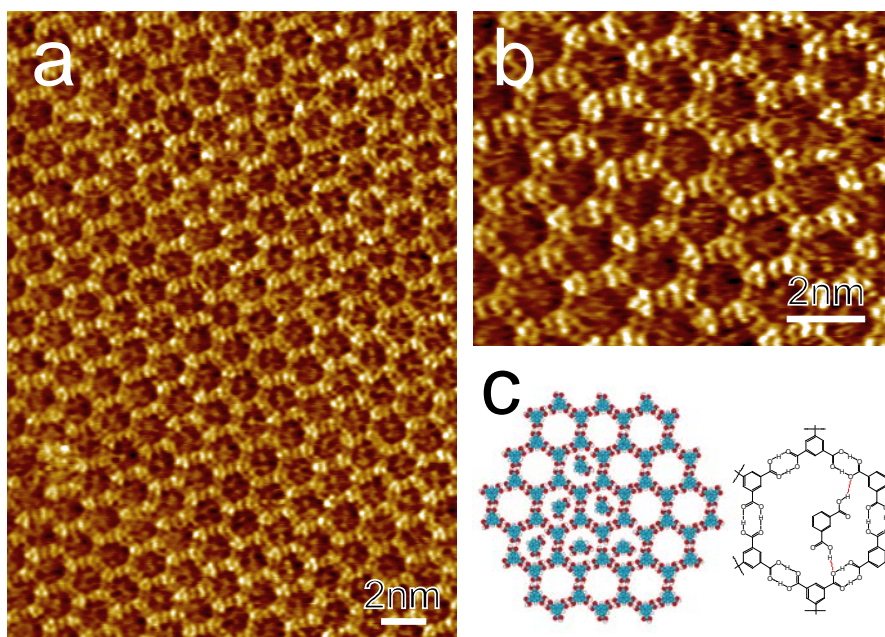


Figure S3. Large scale (a) and high resolution (b) STM images of the host-guest network formed by codeposition of **TMA** and **ISA** at the 1-octanoic acid/graphite interface from saturated solutions. A **TMA** network is formed, hosting some **ISA** molecules. (c) Left: Tentative model of the **TMA** network with some trapped **ISA** molecules. Right: H-bond network and stabilization of trapped **ISA** in a pore of the **TMA** network. $I_{\text{set}} = 575 \text{ pA}$, $V_{\text{set}} = -1.02 \text{ V}$.

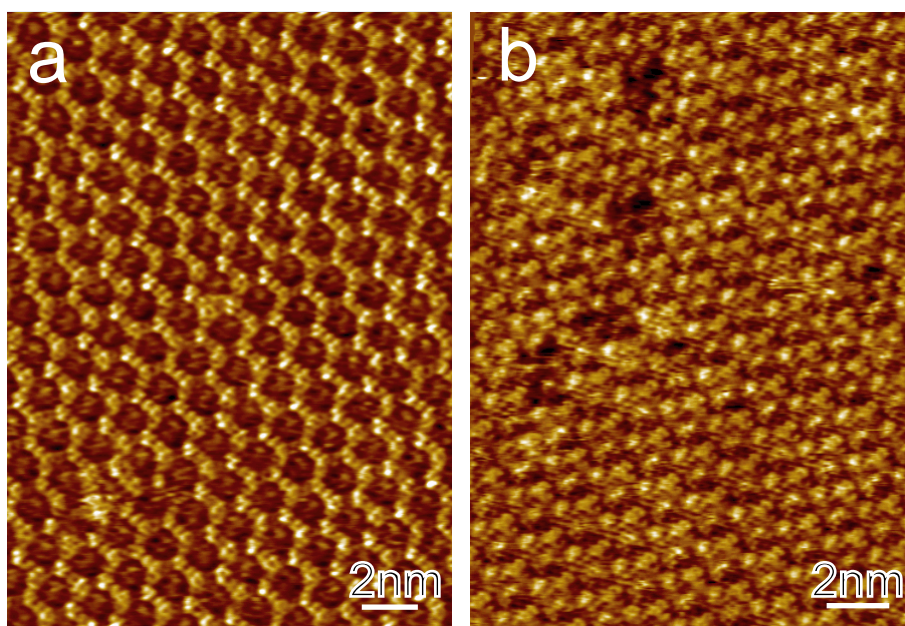


Figure S4. Consecutive STM images of the same area of the **TMA/ISA** co-assembly at the 1-octanoic acid/graphite interface. (a) $I_{\text{set}} = 619$ pA, $V_{\text{set}} = -1.00$ V. (b) $I_{\text{set}} = 855$ pA, $V_{\text{set}} = -1.00$ V. The **ISA** guest molecules are revealed more clearly compared to that obtained at low tunneling current but are hardly distinguishable from the **TMA** molecules.

B.5. Assembly of ternary mixture of TMA, ISA and COR

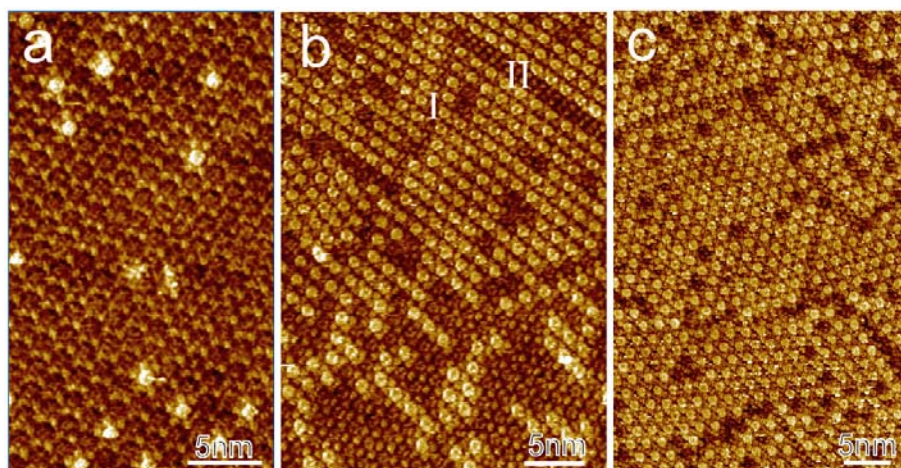


Figure S5. STM snapshots of different stages of the dynamic assembly of the ternary mixture of **TMA/ISA/COR** (a) 20 minutes after deposition ($I_{\text{set}} = 575$ pA, $V_{\text{set}} = -1.04$ V) (b) 1 hour after deposition ($I_{\text{set}} = 305$ pA, $V_{\text{set}} = -1.04$ V) (c) 5.5 hours after deposition ($I_{\text{set}} = 530$ pA, $V_{\text{set}} = -1.00$ V). Initially, only the **TMA** network hosting **ISA** and a few **CORs** are observed. In time, the **ISA** guest is replaced by **COR**. Some domain boundaries are created by replacement of host **TMA** by **ISA** (as marked as I and II, see Figure S6 for high-resolution images). Note that the replacement of **TMA**

by **ISA** only occurs between **COR** filled domains.

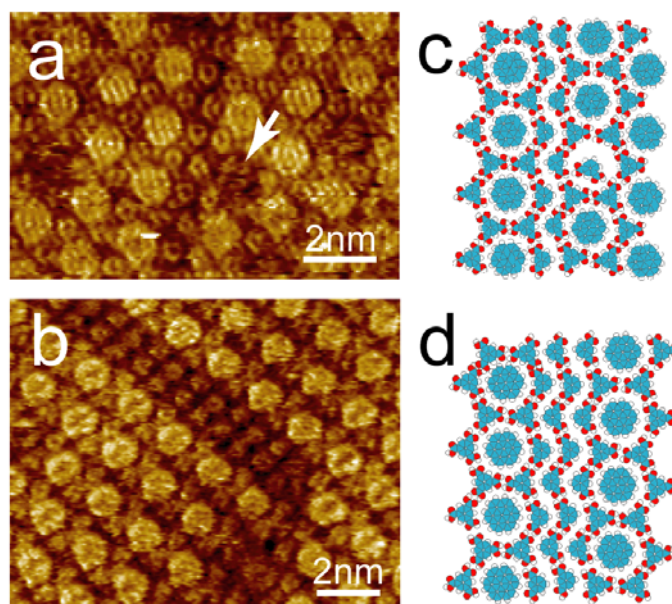


Figure S6. STM images of monolayers formed from a mixture of **TMA/ISA/COR** at the 1-octanoic acid/graphite interface at a late stage of the self-assembly. (a,b) Two type of domain boundaries created by insertion of **ISA** in the **TMA** network (marked as I and II in Figure S5b) ($I_{\text{set}} = 205 \text{ pA}$, $V_{\text{set}} = -1.04 \text{ V}$) and (c,d) corresponding molecular models of these domain boundaries. The white arrow in (a) highlights a cavity in which a **ISA** molecule is trapped.

B.6. Assembly of **DBA1** in the presence of **TMA** and **COR**

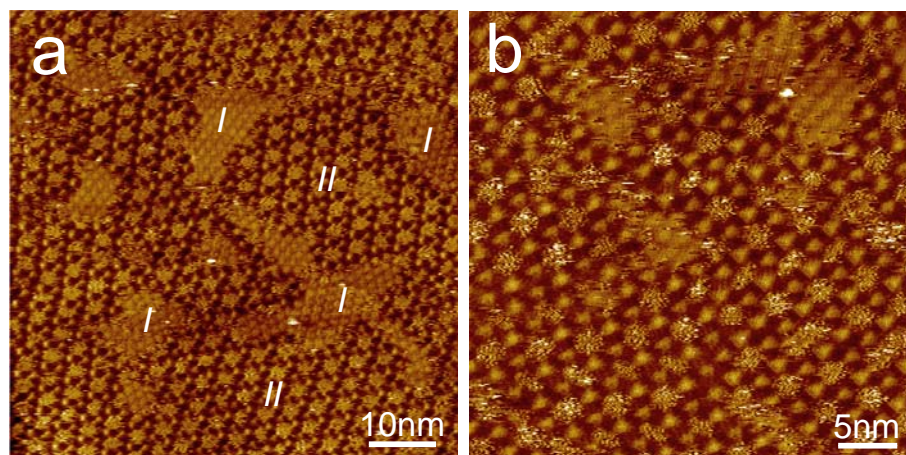


Figure S7. STM images of monolayers formed from a solution of **TMA/COR** and **DBA1** at the 1-octanoic acid/graphite interface. Two different kinds of domains are observed, which are marked as I and II in (a). Domain I is a host-guest pattern of **TMA** and **COR**, while domain II is a host-guest pattern of **DBA1** and **COR**. In domain II the **COR** guest molecules are mobile due to the mismatch of the guest and pore size. No **TMA-COR** clusters are stabilized in the **DBA1** cavities. ($I_{\text{set}} = 356 \text{ pA}$, $V_{\text{set}} = 0.53 \text{ V}$)

C. Molecular Mechanics and Molecular Dynamics Simulations

C.1. Molecular Modeling methodology

Molecular modeling calculations and analysis of the results were performed using the Materials Studio 4.0 and Cerius2 packages from Accelrys. The atomic charges were assigned by the PCFF force field, which were in good agreement with high-level quantum-chemical calculations and therefore used as such in Molecular Mechanics (MM) calculations. Geometry optimization was carried out using the PCFF force field, which provides an accurate description of organic and polymeric systems.² Alternatively, we used the generic force field Dreiding for the description of H-bonds, as it contains explicit H-bond parameters together with a relatively good description of the geometry of organic systems.³ We used the Conjugate Gradient algorithm with an RMS Force convergence parameter set to 10^{-2} kcal/mol.Å and the non-bonded van der Waals and electrostatic terms were described by a Spline function, with a cut-off at 14.0 Å (Spline width: 3 Å). For calculating the interactions with a graphite surface, we used the same methodology than that applied for a phenylene-ethynylene macrocycle,⁴ i.e., using a two-sheet periodic cell with electrostatic interactions treated with the Ewald technique (accuracy of 0.01 kcal/mol). Molecular Dynamics (MD) was performed in the canonical ensemble (N,V,T) at 298 K with a Nosé-Hoover thermostat. The time step was set to 1 fs and the duration of the MD run was 300 ps, with an output frame collected every 150 fs.

C.2. Table

Table: Some relevant energies, as estimated by the PCFF force field, in kcal/mol.

| Multimolecular system (without graphite) | $E_{b, \text{guest}}^{(1)}$ |
|---|--|
| 6 ISA + COR | GUEST= COR : -13.0 |
| 6 DBA1 + 6 ISA&Cor | COR ₁ -ISA ₆ : -17.7 |

| Molecule adsorbed on graphite | $E_{\text{adsorption}}^{(2)}$ |
|------------------------------------|-------------------------------|
| ISA | -17.3 |
| COR | -33.4 |
| C ₁₀ H ₂₁ OH | -20.8 |
| DBA1 | -173.4 |

(1) The binding energy of the GUEST is here defined as : $E_{b, \text{guest}} = E_{\text{tot}} - E_{\text{cluster}} - E_{\text{guest}}$

where E_{tot} is the energy of the whole system, E_{cluster} is the energy of the cluster without the GUEST system, and E_{guest} is the energy of the isolated GUEST. Note that the interaction with graphite is not taken into account.

(2) The adsorption energy is defined as : $E_{\text{ads}} = E_{\text{tot}} - E_{\text{subst}} - \sum E_{\text{molec}}$

where E_{tot} is the energy of the whole system, E_{subst} is the energy of the graphite lattice, and E_{molec} is the energy of the isolated molecule.

C.3. The pure ISA monolayer : linear vs. hexagonal H-bonded networks

Here we calculate the interaction energy between the two observed forms of packing of **ISA** on graphite: the linear network (pure **ISA**) vs. the hexagonal network (occurring when **COR** is added to the solution). We consider six molecules in each case, in the packing geometry shown in Figure S8. Note that the so-called *linear* network depicts in fact a zig-zag H-bonding network (Figure S8, left).

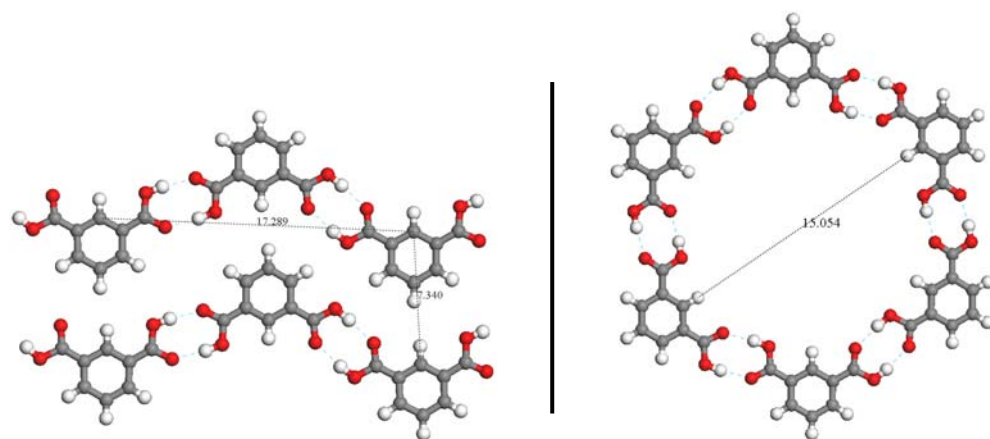


Figure S8. Zig-zag (left) and cyclic hexamer (right) H-bonding networks formed by six **ISA** molecules. The H-bonds are shown by dashed light blue lines.

C.4. The two-component monolayer : **COR/ISA**

Figure S9 shows the energy minimized-structure of a **COR₁-ISA₆** cluster on graphite (two sheets made of 30×30 unit cells). Clearly, all the molecular planes are parallel to the graphite sheets, at a distance of around 3.6 Å to the first graphite plane. The distance between the molecules clearly fits with what has been observed in STM, i.e. a distance between adjacent **ISA** centers of 9.9 Å (STM estimation : 0.96 ± 0.05 nm). **COR**, which can be viewed as a small piece of graphite, adopts an “epitaxial” configuration compared to the first graphite plane. The binding energy between **COR** and the network formed by the six **ISA** molecules (without taking into account the interaction with graphite) is estimated to be −13.0 kcal/mol using the PCFF force field.⁵ This is to be compared to the adsorption energy of a single **COR** on graphite, i.e. −33.4 kcal/mol (see note⁶). In total, the binding energy of **COR** in the system “**ISA** network + **COR** on graphite surface” is rather large, i.e. −46.4 kcal/mol.

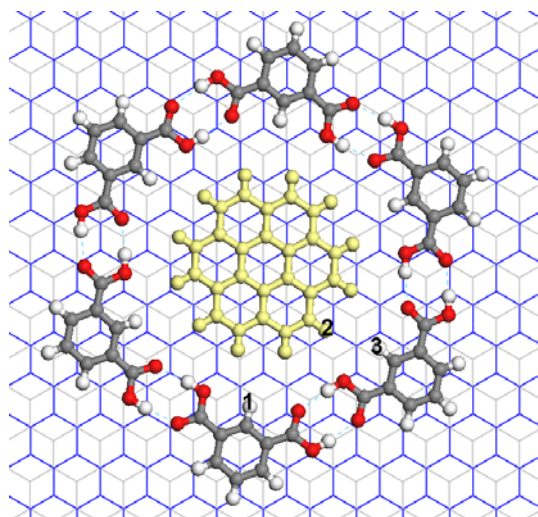


Figure S9: “Ball and stick” molecular model of **COR** (yellow) inside a **ISA** hexamer. The top graphite plane is shown in blue and the underneath sheet is in light gray.

Molecular Dynamics (using the Dreiding force field), maintaining the position of the

ISA molecules in their initial H-bonding network, shows that **COR** has very restricted mobility in the cavity. The standard deviation on distances between **ISA** and **COR** during the MD, for instance on distance between atoms 2 and 3 in Figure S10 (average distance = 3.0 Å) is only ± 0.2 Å. MD shows no rotation of **COR** inside the cavity. This is illustrated in Figure S10, showing the evolution of the angle 1-2-3 (as depicted in Figure S9) during the MD simulation: this angle remains almost constant during the whole MD run, with an average at $114.2^\circ (\pm 6.1^\circ)$.

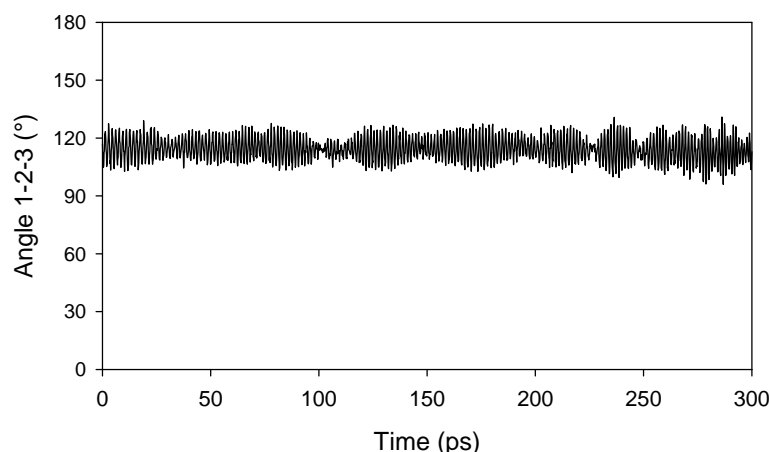


Figure S10. Evolution of the angle formed by atoms 1-2-3 (shown in Fig. S10) during the MD run.

C.5. The three-component monolayer: DBA/COR/ISA

The CPK molecular model in Figure S11 shows the minimized structure obtained after construction of the three-component lattice (adsorbed on a two-sheet made graphite surface of 55×55 unit cells). This packing is very stable, as it combines π -stacking of the core and C-H – π interactions of the alkyl groups on graphite (some alkyl groups showing an epitaxial ordering with respect to the substrate lattice). The binding energy between the **DBA1** network and a **COR₁-ISA₆** cluster, i.e., the energy required to remove the heterocluster from the **DBA1** network ignoring the interaction with graphite, amounts to -17.7 kcal/mol, as estimated using PCFF. Such quite large binding energy illustrates the high stability of this three-component lattice.

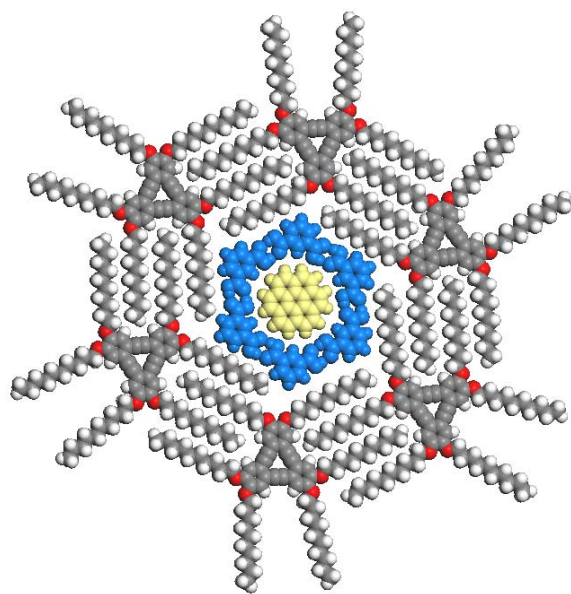


Figure S12. CPK molecular model of the three-component monolayer. **DBA1** molecules are colored by element, **ISA** molecules are shown in blue, and **COR** in yellow. The graphite surface underneath is not shown for the sake of clarity.

References

- ¹ Tahara, K.; Furukawa, S.; Uji-I, H.; Uchino, T.; Ichikawa, T.; Zhang, J.; Mamdouh, W.; Sonoda, M.; De Schryver, F. C.; De Feyter, S.; Tobe, Y. *J. Am. Chem. Soc.* **2006**, *128*, 16613
- ² (a) Sun, H.; Mumby, S.J.; Maple, J.R.; Hagler, A.T. *J. Am. Chem. Soc.*, **1994**, *116*, 2978. (b) Sun, H.; Mumby, S.J.; Maple, J.R.; Hagler, A.T. *J. Phys. Chem.* **1995**, *99*, 5873. (c) Sun, H. *Macromolecules* **1995**, *28*, 701. (d) Sun, H. *J. Comput. Chem.* **1994**, *15*, 752.
- ³ Mayo, S.L.; Olafson, B.D.; Goddard III, W.-A. *J. Phys. Chem.* **1990**, *94*, 8897.
- ⁴ A. Ziegler, W. Mamdouh, A. Ver Heyen, M. Surin, H. Uji-i, M.M.S. Abdel-Mottaleb, F. C. De Schryver, S. De Feyter, R. Lazzaroni, S. Höger, *Chem. Mater.* **2005**, *17*, 5670.
- ⁵ This is at variance with what has been proposed by Griessl et al. [*Langmuir* **2004**, *20*, 9403], who calculated an interaction energy of -54 kcal/mol. However, no detail of the calculation procedure is given in that article.
- ⁶ Zacharia et al. [*Phys. Rev. B* **2004**, *69*, 155406] have measured the desorption energy of coronene on graphite, by means of Thermal Desorption experiments. They measured an activation energy of 1.40 eV (32.3 kcal/mol), which is very close to the adsorption energy of coronene on graphite estimated by PCFF (33.4 kcal/mol), clearly illustrating the reliability of our modeling approach. However, Dreiding overestimates the non-bonded energies, with a binding energy value around -50 kcal/mol. Note that the experimental value is anyway larger than the force-field estimated total binding energy with the **ISA** hexagonal network.